PHYSICAL REVIEW B, VOLUME 63, 220502(R)

Crystallization of the ordered vortex phase in high-temperature superconductors

D. Giller, B. Ya. Shapiro, I. Shapiro, A. Shaulov, and Y. Yeshurun
Institute of Superconductivity, Department of Physics, Bar-Ilan University, Ramat Gan 5290, Israel
(Received 9 November 2000; published 3 May 2001)

The Landau-Khalatnikov time-dependent equation is applied to describe the crystallization process of the ordered vortex lattice in high-temperature superconductors after a sudden application of a magnetic field. Dynamic coexistence of a stable ordered phase and an unstable disordered phase, with a sharp interface between them, is demonstrated. The transformation to the equilibrium ordered state proceeds by movement of this interface from the sample center toward its edge. The theoretical analysis dictates specific conditions for the creation of a propagating interface and provides the time scale for this process.

DOI: 10.1103/PhysRevB.63.220502 PACS number(s): 74.60.Ge, 64.60.My, 05.70.Fh, 64.60.Cn

The process of formation of various equilibrium phases after a sudden change in the thermodynamic conditions is a topic of wide theoretical[1] and experimental[2] interest. Obviously, the initial state created immediately after the abrupt change is a nonequilibrium, unstable state. The transformation of this state to the thermodynamic equilibrium state may proceed either homogeneously throughout the entire system or by nucleation of a spatially localized domain of the equilibrium phase, creating a front that propagates until equilibrium is reached in the entire system. The latter process has been recently observed in the vortex system of $Bi_2Sr_2CaCu_2O_{8+\delta}$ (BSCCO) crystals.[3,4] This vortex system exhibits a transition between ordered and disordered phases at a temperature-independent transition field $B_{od} \simeq 400$ G.[5,6] High temporal resolution magnetooptical measurements[3,4] indicated that immediately after a sudden application of external magnetic field $B_a \lesssim B_{od}$, a transient disordered vortex state is created, followed by a nucleation and front propagation of an ordered vortex state.[3] The purpose of this paper is to analyze theoretically the crystallization process of the vortex ordered phase, i.e., the nucleation process and the creation of a front and its motion.

Our analysis is based on the Landau-Khalatnikov (LK) time-dependent equation[7]

$$\frac{\partial \Psi}{\partial t} = -\Gamma \frac{\delta F}{\delta \Psi}, \tag{1}$$

where Ψ and F are the order parameter and the free energy of the system, respectively, and Γ is the Landau-Khalatnikov damping coefficient. We define the order parameter of the vortex system in a way analogous to the definition of the order parameter in order-disorder transitions in atomic solids.[8] In the latter case, the order parameter ρ_q is a set of Fourier components of the atomic density taken at reciprocal-lattice vectors $q=G$. In particular, for an ordered lattice phase $\rho_q = \text{const} \neq 0$ at $q=G$, whereas for a disordered state $\rho_q = 0$ for all $q \neq 0$. Extending this approach to the vortex order-disorder phase transition, we note that in small-angle neutron-scattering experiments in BSCCO,[5] Bragg peaks are observed at low temperatures and low fields mainly in the first Brillouin zone; these peaks are smeared for fields larger than B_{od}. Thus, only one component ρ_{G_1} is sufficient to completely describe the order parameter, ρ_{G_1} being the value of the Fourier component of the *vortex* density at the minimal vector of the reciprocal lattice. In order to describe the kinetics of the phase transition we allow the order parameter to be temporally and spatially dependent $\Psi(\mathbf{r},t) \equiv \rho_{G_1}(\mathbf{r},t)$, assuming that $\Psi(\mathbf{r})$ varies slowly over the intervortex distance. The scalar real order parameter $\Psi(\mathbf{r},t)$ so defined, distinguishes between two thermodynamic solid phases of the vortex matter: $\Psi=0$ for the disordered state and $\Psi=\Psi_0 \neq 0$ for the ordered state.

In the Ginzburg-Landau formalism, the phase transition between the ordered and disordered phases may be described by a free-energy density functional F

$$F = \frac{1}{2} D(\nabla \Psi)^2 - \frac{1}{2}\alpha \Psi^2 - \frac{1}{3}\beta \Psi^3 + \frac{1}{4}\gamma \Psi^4, \tag{2}$$

where α, β, γ, and D are the Landau coefficients. These coefficients depend on the vortex-vortex and vortex-pinning interactions, and their evaluation requires a microscopic theory that does not yet exist. Note that Eq. (2) does not describe the whole free energy of the vortex system, but only that part that is varying through the phase transition, i.e., Ψ dependent.

As the order-disorder vortex phase transition in BSCCO is field driven, we express the parameter α as a function of B,

$$\alpha = \alpha_0 (1 - B/B^*), \tag{3}$$

where B^* is a characteristic field related to the transition field $B_{od} = B^*(1+2/9\mu)$, where $\mu = \alpha_0 \gamma / \beta^2$. Note that for a second-order transition ($\beta=0$), $B_{od}=B^*$. For a first-order phase transition, metastable states of the system are found between B^* and $B^{**} = B^*(1+1/4\mu)$. For $B<B^*$ the disordered state is unstable while the ordered state, characterized by

$$\Psi = \Psi_0 = \frac{\beta}{2\gamma}\left[1 + \sqrt{1 + 4\mu(1 - B/B^*)}\right],$$

is stable. For $B>B^{**}$ the ordered state is unstable, while the disordered state with $\Psi=0$ is thermodynamically favorable. All the above results are deduced from the conventional Landau theory for phase transitions[9] by replacing temperature with the induction B.

In solving Eq. (1) we assume an initial nonequilibrium disordered vortex state ($\Psi=0$) caused by the rapid injection of the vortices through nonuniform surface barriers.[3,11] We show that Eq. (1) can describe the nucleation and growth of the vortex ordered state ($\Psi=\Psi_0$). To demonstrate this point we assume an induction distribution with a constant gradient[10] $\tilde{B}/d$, i.e., $B=B_a-\tilde{B}(1-|x|/d)$, where d is half-width of the sample and B_a is the applied field. In this case, Eq. (1) can be solved analytically for both the nucleation and growth processes.

A solution for the nucleation process, i.e., the *initial* growth of the order parameter Ψ (Ψ close to zero), is obtained by neglecting nonlinear terms in Eq. (1),

$$\frac{1}{\Gamma}\frac{\partial\Psi}{\partial t}=D\frac{\partial^2\Psi}{\partial x^2}+\left(\alpha_0-\alpha_0\frac{B_a-\tilde{B}}{B^*}-\alpha_0\frac{\tilde{B}}{B^*}\frac{x}{d}\right)\Psi. \quad (4)$$

The boundary conditions dictated by symmetry are $d\Psi(x,t)/dx|_{x=0}=0$; also we require that $\Psi(x,t)$ is a nondiverging function. The solution of Eq. (4) is then

$$\Psi(x,t)=\sum_{n=0}^{\infty}A_n e^{\Lambda_n t}\,\mathrm{Ai}(x/x_s-\varsigma_n), \quad (5)$$

where

$$\Lambda_n=\Gamma\alpha_0\left[1-\frac{B_a-\tilde{B}}{B^*}-\varsigma_n\left(\frac{a_D}{\mu}\right)^{1/3}\left(\frac{\tilde{B}}{B^*}\right)^{2/3}\right]. \quad (6)$$

Ai is the Airy function, $\varsigma_n=0.685,3.9,7.06,\ldots$ are the solutions of $J_{2/3}(\varsigma_n)=J_{-2/3}(\varsigma_n)$ where J_ν is the Bessel function, and $x_s=(DdB^*/\alpha_0\tilde{B})^{1/3}=d(a_DB^*/\mu\tilde{B})^{1/3}$. Here $a_D=D\gamma/\beta^2d^2$ is a dimensionless exchange coefficient. Note that ς_n is a constant of order n, growing with increasing n.

It is evident from Eq. (5) that only terms with $\Lambda_n>0$ play a role in the nucleation process. For $B_a-\tilde{B}>B^*$, i.e., the entire sample is in a metastable or a stable state, all Λ_n are negative, implying that the nucleation process cannot take place. For $B_a=\tilde{B}$ the induction at the center of the sample is zero and the rate of the nucleation process is maximum. Relation (6) shows that the exponent with $n=0$ yields the fastest nucleation rate, thus governing the nucleation process. This process may thus be approximately described by the first term in Eq. (5). In this approximation, the development of the order parameter during the nucleation process is described by the dashed lines in Fig. 1. Note that the analytical solution (5) describes only the first stages of the nucleation process, where the nonlinear terms in Eq. (1) may be neglected. This solution ceases to apply when the value of Ψ approaches Ψ_0, i.e., after a time period of order $1/\Lambda_0$. The width of the ordered domain is then $w\sim x_s(1+\varsigma_0)\sim x_s$. The condition for appearance of a *localized* domain in the sample center may be then obtained from the inequality $x_s\ll d$ or

$$\frac{\tilde{B}}{B^*}\gg\frac{a_D}{\mu}. \quad (7)$$

If this condition is not satisfied, then *homogeneous* transformation of the unstable phase takes place. Otherwise, a sharp *front* will develop separating between the nucleating ordered phase and the initial unstable disordered phase, as described above. Thus, when the induction gradient is large enough, we expect the appearance of a sharp interface between the growing stable (ordered) phase and the retreating unstable (disordered) phase.

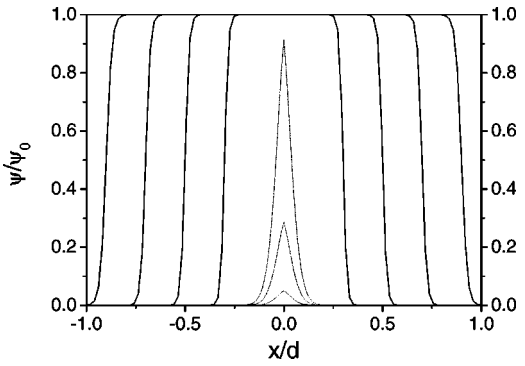

FIG. 1. Nucleation and growth of the order parameter. The nucleation process is demonstrated by the dashed curves calculated from Eq. (5) for $A_n=A_0\delta_{n,0}$ at times $\Lambda_0 t=8.12$, 9.86, 11.02. The solid lines, describing the growth process, are calculated from Eq. (9) at different locations $x_f/d=0.3$, 0.5, 0.7, 0.9.

In describing the *growth* process, i.e., the movement of the interface between the ordered and disordered phases, nonlinear terms in Eq. (1) must be taken into account. We express the linearly varying function $B(x)$ as $B=B_f+(\tilde{B}/d)(x-x_f)$, where $B_f=(B_a-\tilde{B})+x_f\tilde{B}/d$ is the induction at the front located at x_f. In this notation $\alpha=1-[B_f+(\tilde{B}/d)(x-x_f)]/B^*$. Eq. (1) can be written in the reference frame of an observer moving with the front by introducing a new variable $\xi=x-x_f(t)$ and defining $x_f(t)\equiv x_0+\int_0^t v_f(t')dt'$, where v_f is the time-dependent front velocity and x_0 is a constant. With the new set of independent variables (ξ,B_f) Eq. (1) becomes

$$\frac{v_f}{\Gamma}\left(-\frac{\partial\Psi}{\partial\xi}+\frac{\tilde{B}}{d}\frac{\partial\Psi}{\partial B_f}\right)=D\frac{\partial^2\Psi}{\partial\xi^2}+\alpha_0\left(1-\frac{B_f\{x_f(t)\}}{B^*}-\frac{\tilde{B}\xi}{dB^*}\right)\Psi+\beta\Psi^2-\gamma\Psi^3. \quad (8)$$

One can solve this equation analytically provided the front width $\Delta\ll dB_f/\tilde{B}$. In this case, the terms $(v_f/\Gamma)(\tilde{B}/d)(\partial\Psi/\partial B_f)$ and $-\alpha_0(\tilde{B}\xi/dB^*)\Psi$ may be neglected.[12] The solution of Eq. (8) is then[13]

$$\Psi=\Psi_0\left\{1+\exp\left(\frac{\xi}{\Delta}\right)\right\}^{-1}, \quad (9)$$

where

$$\Delta^2=\frac{\Delta_0^2}{2\mu(1-B_f/B^*)+1+\sqrt{1+4\mu(1-B_f/B^*)}} \quad (10)$$

is the front width. The front velocity $v_f=dx_f/dt$ is

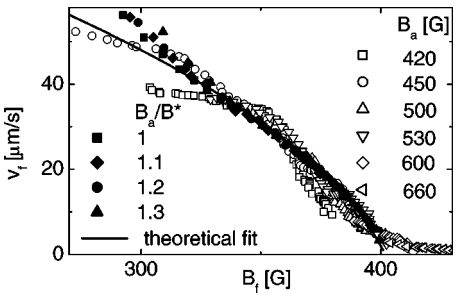

FIG. 2. Experimental data (open symbols) of $v_f(B_f)$ for different applied fields taken from Ref. 3, a fit (solid line) to Eq. (11), and results of numerical solutions (solid symbols) for the indicated applied fields. The fit was done with two fitting parameters v_0 and μ, after B_{od} was estimated to be approximately 400 G, corresponding to an induction value where the velocity is going to zero.

$$v_f = v_0 \frac{6\mu(1-B_f/B^*)+1+\sqrt{1+4\mu(1-B_f/B^*)}}{\sqrt{2\mu(1-B_f/B^*)+1+\sqrt{1+4\mu(1-B_f/B^*)}}}. \tag{11}$$

Here

$$v_0 = \Gamma\sqrt{D\beta^2/4\gamma} = \Gamma\alpha_0 d\sqrt{a_D}/2\mu, \quad \Delta_0^2 = 4D\gamma/\beta^2 = 4d^2 a_D, \tag{12}$$

and $B_f \equiv B_f\{x_f(t)\}$. The solid lines in Fig. 1 show Ψ given in Eq. (9) for different locations of the front x_f, describing the propagation of the ordered phase.

We turn now to discuss the front velocity v_f, Eq. (11), and the front width Δ, Eq. (10). We first note that v_f and Δ do not depend *explicitly* on time or applied field but on B_f, the *local* induction at the front. Several important conclusions may be drawn from these equations:

(1) As B_f approaches B_{od} the velocity approaches zero [the $v_f(B_f)$ dependence is described by the solid line in Fig. 2].

(2) The motion of the front toward the sample edge is accompanied by an increase in the induction B_f at the front, resulting in a decrease in the velocity with time.

(3) The front width Δ decreases with the increase of β, implying that for a ''stronger'' first-order transition the front is steeper. Also from Eq. (10) it is obvious that the exchange coefficient D causes the front to be smeared. In addition, increasing D and/or the damping coefficient Γ results in an acceleration of the front motion [see Eq. (11)].

So far we have demonstrated dynamic coexistence of ordered and transient disordered vortex phases, with a sharp interface between them, assuming a time-independent induction distribution with a constant gradient. In high-temperature superconductors, however, the induction distribution varies significantly with time due to flux creep. In addition, one may expect different flux creep laws for the different vortex phases. As a result, the nucleation and growth of the ordered vortex phase are manifested experimentally by the appearance of a break in the induction profile and movement of this break toward the sample edge.[3] The location of the break is expected to coincide with the location of the moving front of the order parameter.

To demonstrate this scenario we solved numerically the LK Eq. (1), allowing for flux creep. We assume a Ψ-dependent local current density

$$J(\Psi,t) = J_1(t)\left(1-\frac{\Psi}{\Psi_0}\right) + J_2(t)\frac{\Psi}{\Psi_0}, \tag{13}$$

where $J_1(t)$and $J_2(t)$ are the current densities in the disordered and in the ordered phases, respectively.[14] Based on the experimental observations[3] we further assume $J_1(t) = J_{01}(1+t/t_1)^{-\alpha_1}$ and $J_2(t) = J_{02}(1+t/t_2)^{-\alpha_2}$. The induction B (and thus the coefficient α) may now be expressed in terms of the order parameter $\Psi(x)$ by using the Maxwell equation $B(x,t) = B_a - 4\pi/c\int_x^d J(\Psi(y,t),t)dy$. As before, we assume an initial disordered phase throughout the entire sample $\Psi(t=0,x)=0$.

In order to solve Eq. (1) numerically we define dimensionless parameters: $b = B/B^*$, $j = 4\pi J d/(cB^*)$, $x' = x/d$, $t' = t\beta^2\Gamma/\gamma$, and $\Psi' = \Psi/\Psi_0(B^{**}) = 2\Psi\gamma/\beta$. Equation (1) then becomes

$$\frac{\partial\Psi'}{\partial t'} = a_D\frac{d^2\Psi'}{dx'^2} + \mu[1-b(x')]\Psi' + \frac{1}{2}\Psi'^2 - \frac{1}{4}\Psi'^3 + f'(\mathbf{x}',t'), \tag{14}$$

where $f' = 2f\gamma/(\beta\alpha_0)$ is a dimensionless noise that must be introduced in the numerical solution.

The values of the (dimensionless) parameters used in the numerical calculations are based on experimental measurements. In particular, from the fit of Eq. (11) to the experimental data[3] of $v_f(B_f)$ in Fig. 2 we estimate $\mu = 1.5$, thus

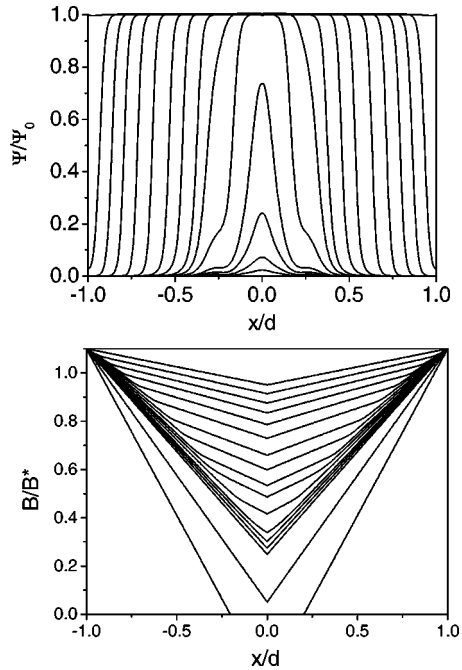

FIG. 3. Order parameter (upper case) and induction profiles (lower case) for $j_1 = 1.7(1+t')^{-0.3}$ and $j_2 = 1.5(1+t')^{-0.5}$. The profiles are shown for dimensionless times $t' = 1$, 4, 9, 10, 11, 12, 14, 16, 18, 22, 27, 35, 44, 54, 65, 79, 99.

$B_{od}/B^*=1.148$, $B^{**}/B^*=1.166$. A value of 10^{-4} for $a_D=[2\mu v_0/(\Gamma\alpha_0 d)]^2$ [see Eq. (12)] is estimated from the experimental value $v_0\approx 20$ μm/s obtained from the same fit; a value of $\Lambda_0\sim\Gamma\alpha_0\approx 10$ s^{-1} is estimated from the time elapse between switching on the external field and the appearance of a break in the induction profile. A typical value of $d\approx 300$ μm for the sample half-width was used. Based on the analysis of magnetic relaxation we take $\alpha_1=0.3$, $\alpha_2=0.5$. In addition, a noise level of $f'_{\max}=10^{-4}$ is assumed. The system of equations completed by boundary and initial conditions has been solved numerically utilizing the Euler method. The unit space interval was divided into 200 segments, and a time step of 2.5×10^{-3} (in dimensionless units) was used providing a stability of the numerical procedure. The results for $B_a/B^*=1.1$ are shown in Fig. 3. The upper case shows the spatial dependence of the order parameter at different times. The nucleation appears at the sample center at $t'\sim 10$, forming a sharp front that propagates toward the sample edge.[15] The lower case of Fig. 3 shows the time evolution of the induction profiles during the nucleation and growth processes. A sharp break in the profiles appears at the location of the front of the order parameter after the nucleation is completed. As expected, the break in the induction profile and the front of the order parameter move together toward the sample edge. Note that a break in the induction profile can be observed outside the region of phase metastability (i.e., for $B_f<B^*$).

The theoretical predictions described above are confirmed experimentally in BSCCO crystals.[3] In particular, breaks in the induction profiles were recorded following a sudden application of external field of intensity close to B_{od}. This break moves toward the sample edge at a velocity that depends only on B_f, the value of the induction at the break. Thus, the dependence of v_f on B_f is not affected by magnetic relaxation. As shown in Fig. 2, the *analytical* curve (solid line) of $v_f(B_f)$, Eq. (11), is in good agreement with the experimental results (open symbols). Moreover, numerical results (solid symbols in Fig. 2) for $v_f(B_f)$ for different applied fields also show a good agreement with the analytical curve demonstrating that magnetic relaxation does not affect the dependence of v_f on B_f.

Finally, we note that two velocities govern the vortex dynamics in the process of the phase transformation: The interface velocity v_f and the flux velocity v_F, due to creep. The effect of the latter on the shape of the interface must be taken into account in close vicinity of B_{od} where $v_f\to 0$.

This research was supported by The Israel Science Foundation founded by the Israel Academy of Sciences and Humanities–Center of Excellence Program, and by the Heinrich Hertz Minerva Center for High Temperature Superconductivity. Y.Y. acknowledges support from the U.S.-Israel Binational Science Foundation. D.G. acknowledges support from the Clore Foundation.

[1] S. Dorfman *et al.*, Phys. Rev. B **52**, 12 473 (1995); **52**, 7135 (1995); S.J. Di Bartolo and A.T. Dorsey, Phys. Rev. Lett. **77**, 4442 (1996); T.W.B. Kibble and G.E. Volovik, Pis'ma Zh. Éksp. Teor. Fiz. **65**, 96 (1997) [JETP Lett. **65**, 102 (1997)]; N.B. Kopnin and E.V. Thunenberg, Phys. Rev. Lett. **83**, 116 (1999); Wim van Saarloos, Phys. Rep. **301**, 9 (1998), and references therein.

[2] P.E. Cladis *et al.*, Phys. Rev. Lett. **62**, 1764 (1989); M.A. Anisimov *et al.*, Phys. Rev. A **41**, 6749 (1990); Wang Xin-yi, *ibid.* **32**, 3126 (1985); X.Y. Wang *et al.*, Phys. Rev. Lett. **80**, 4478 (1998); V.M.H. Ruutu *et al.*, Nature (London) **382**, 334 (1996); A.E. Bailey *et al.*, Phys. Rev. E **56**, 3112 (1997).

[3] D. Giller *et al.*, Phys. Rev. Lett. **84**, 3698 (2000); Physica B **284-288**, 699 (2000); Physica C **341-348**, 987 (2000); **341-348**, 1089 (2000).

[4] C.J. van der Beek *et al.*, Phys. Rev. Lett. **84**, 4196 (2000).

[5] R. Cubitt *et al.*, Nature (London) **365**, 407 (1993).

[6] S.L. Lee *et al.*, Phys. Rev. Lett. **71**, 3862 (1993); B. Khaykovich *et al.*, *ibid.* **76**, 2555 (1996); M.B. Gaifullin *et al.*, *ibid.* **84**, 2945 (2000).

[7] See, for example, L.D. Landau and I.M. Khalatnikov, Dokl. Akad. Nauk SSSR **96**, 469 (1954). [English translation in *The Collected Works of L. D. Landau*, edited by D. ter Haar (Pergamon, Oxford, 1965), pp. 626–633].

[8] R.M. White and T.H. Geballe, *Long Range Order in Solids* (Academic Press, New York, 1979).

[9] P.M. Chaikin and T.C. Lubensky, *Principles of Condensed Matter Physics* (Cambridge University Press, Cambridge, England, 1995).

[10] As shown below, a field gradient is necessary for the creation of front propagation of the equilibrium state.

[11] Y. Paltiel *et al.*, Nature (London) **403**, 398 (2000); Phys. Rev. Lett. **85**, 3712 (2000).

[12] These terms are small in the vicinity of the front and therefore unimportant for the calculation of the front properties. For a similar treatment see, for example, P.C. Fife, J. Chem. Phys. **64**, 554 (1976).

[13] E. Ben-Jacob *et al.*, Physica D **14**, 348 (1985).

[14] A more general approach to this problem should be based on the introduction of different $E(j)$ characteristics for the different phases and a solution of appropriate Maxwell equations. We solved our system using this approach too, and obtained similar results.

[15] The numerical solution does not exhibit breaks in the profiles if the magnetic relaxation is too fast [e.g., $J\sim\exp(-t/t_0)$ while $t_0\ll 1/\Lambda_0$] or if the critical current is too low ($j_{01}\sim j_{02}\lesssim a_D/\mu$). This is because the requirement for a relatively large gradient, mandatory for the front development [Eq. (7)], is not satisfied in these cases. Thus, in $YBa_2Cu_3O_{7-\delta}$, for which $\tilde{B}\ll B_{od}\sim B^*$, a homogeneous phase transformation is expected rather than front propagation.